Beam Physics Note
TRI-BN-24-39
December 17, 2024

Tune measurement and solenoid aberration at e-LINAC

H. W. Koay

TRIUMF

Abstract: This work reports the tune and the corresponding measurements measured using all the VS in the beamline The calculation of the rms beam size was generated using the VS apps. The simulation is compared with results taken on 28th Nov, 2024. The mismatch is suspected to be mainly from the high order aberration at EGUN:SOL1.

1 Introduction

The full layout of the e-LINAC beamline is shown in Fig. 1. 300 keV electron beam is produced at EGUN (on the left in Fig. 1), and accelerated up to ∼30 MeV before dumping it at EHDT:DUMP (on the right).

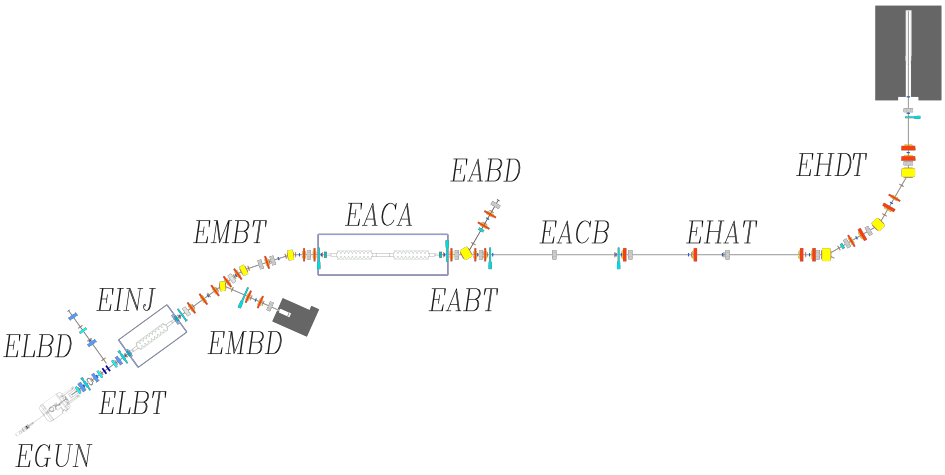

Figure 1: Schematic (top view) of the E-LINAC beamline.

2 Initial condition

Before performing the full comparison of all viewscreens, the initial condition of the beam was determined by performing a fit for solenoid scan (EGUN:SOL1). The fitted results are shown in Fig. 2. Note that X and Y are not symmetry. The fitted data is not exactly 2-rms, but $\sqrt{5}$-rms of the beam.

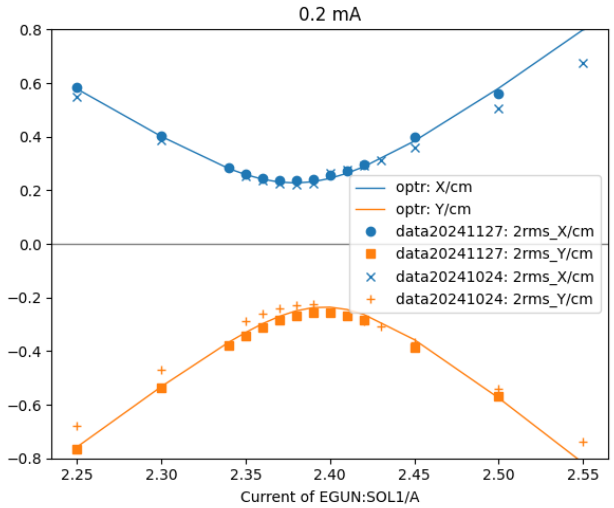

Figure 2: Fitted initial condition in TRASNOPTR.

The initial sigma matrix to be fed into TRANSOPTR at 20 eV is shown below:

```
---Sigma Matrix--------
                    Diagonal       Off-Diagonals (Normalized Form)
 x( cm )            0.320377
 theta( rad)        0.803950       -.790585
 y( cm )            0.515767        0.00000        0.00000
 phi( rad)          0.649318        0.00000        0.00000        -.622640
 l( cm )            0.700000E-02    0.00000        0.00000         0.00000        0.00000
 delta( rad)        0.500000        0.00000        0.00000         0.00000        0.00000
```

3 Comparison with real data

During beam time on Nov 28, 2024, about 200 μA beam was delivered to EHD:DUMP as a preparation for high-power (>1 kW) beam delivery. The cathode heater was set to 5.6 V and the cathode bias was set to 100 V. The beam sizes at all VSs were measured and compared with TRANSOPTR simulations. Again, the envelope data is not exactly 2-rms, but $\sqrt{5}$-rms of the beam. The input values of elements from EGUN to EHD:DUMP are shown in Table 1.

3.1 TRANSOPTR envelope

Results calculated using initial condition defined in Section 2 with element parameters set according to Table 1

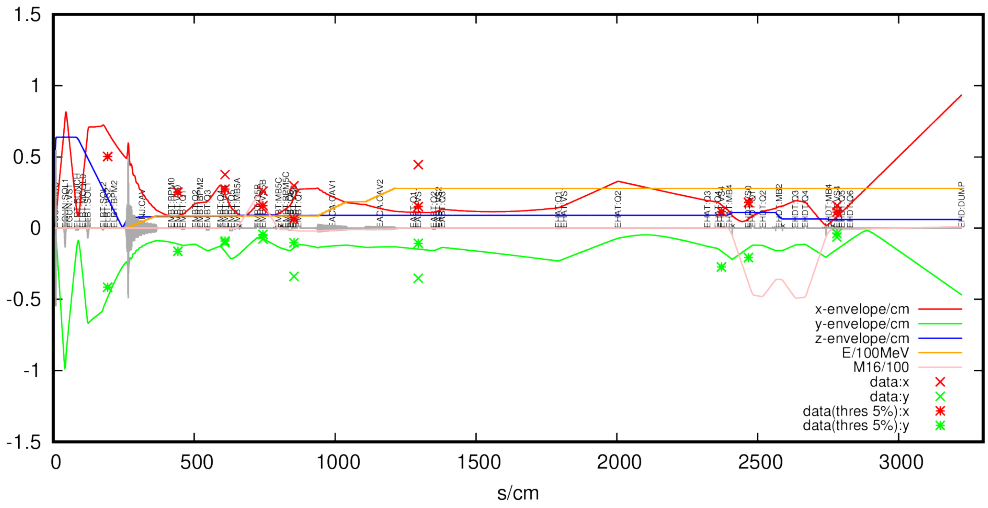

Figure 3: Comparing beam data with TRANSOPTR simulations. The crosses are data processed without any threshold cut, while the stars applied a 5% threshold cut from its maximum value.

Fig. 3 shows a significant mismatch between the data and simulations. The match is slightly improved by applying a 5% threshold cut. This is as if removing the 'halo' from

Value	Item
3e+05	EGUN:BIAS:VOL V1/V
2.91	EGUN:SOL1:CUR B1/A
0.026	ELRF:VVM:BUNCH:BVOL RFA1/V
2.6	ELBT:SOL1:CUR B2/A
1.11	ELBT:SOL2:CUR B3/A
0.186	ELRF:VVM:EINJ:BVOL RFA2/V
-152.2	ELRF:VVM:EINJ:PHASE RFP1/deg
-68.2	ELRF:VVM:BUNCH:PHASE RFP2/deg
-0.6	EMBT:Q1:CUR QM1/A
0.8	EMBT:Q2:CUR QM2/A
-1.0	EMBT:Q3:CUR QM3/A
1.9	EMBT:Q4:CUR QM4/A
-1.3	EMBT:Q5:CUR QM5/A
2.3	EMBT:Q5B:CUR QM6/A
-1.1	EMBT:Q6:CUR QM7/A
1.1	EMBT:Q7:CUR QM8/A
0.6512	ELRF:VVM:EACA1:BVOL RFA3/V
-139.5	ELRF:VVM:EACA1:PHASE RFP3/deg
0.582	ELRF:VVM:EACA2:BVOL RFA4/V
64.6	ELRF:VVM:EACA2:PHASE RFP4/deg
0.0	EABT:Q1:CUR QM9/A
-1.6	EABT:Q2:CUR QM10/A
1.8	EABT:Q3:CUR QM11/A
-2.3	EHAT:Q1:CUR QM12/A
2.1	EHAT:Q2:CUR QM13/A
-0.357	EHAT:Q3:CUR QM14/A
3.614	EHAT:Q4:CUR QM15/A
2.91	EHDT:Q1:CUR QM16/A
3.12	EHDT:Q2:CUR QM17/A
0.0	EHDT:Q5:CUR QM18/A
0.0	EHDT:Q6:CUR QM19/A

Table 1: The values of input elements along e-LINAC beamline. Note that the RF values (ELRF:VVM:XXXX) are the readback picked up from VVM.

the beam. Therefore, it improves slightly the agreement between them. This suggests the potential of a significant aberration propagated from the low energy section of the beam. This deduction is further testified by 'fudging' the current of EGUN:SOL1 from 2.91 A to 3.02 ,A (shown in Fig. 5. The hysteresis from $\int B^2 \mathrm{d}s$ of EGUN:SOL1 was measured to be about ± 0.07 A ($\sim 3 \times 10^5$ G^2 mm) at 2.91 A [1]. Therefore, +0.11 A lies beyond the range of expected hysteresis. This shows the possibility of aberration propagated from the first solenoid.

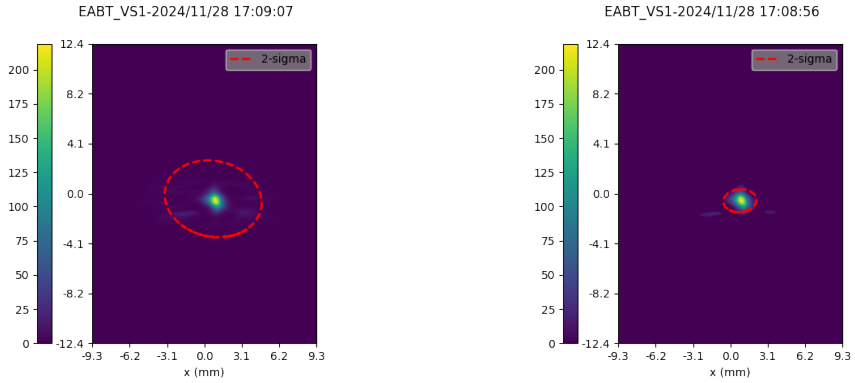

Figure 4: Comparing view screen images. Figure on the left shows the VS image without any threshold cut; while the one on the right has a 5% threshold cut from its maximum values.

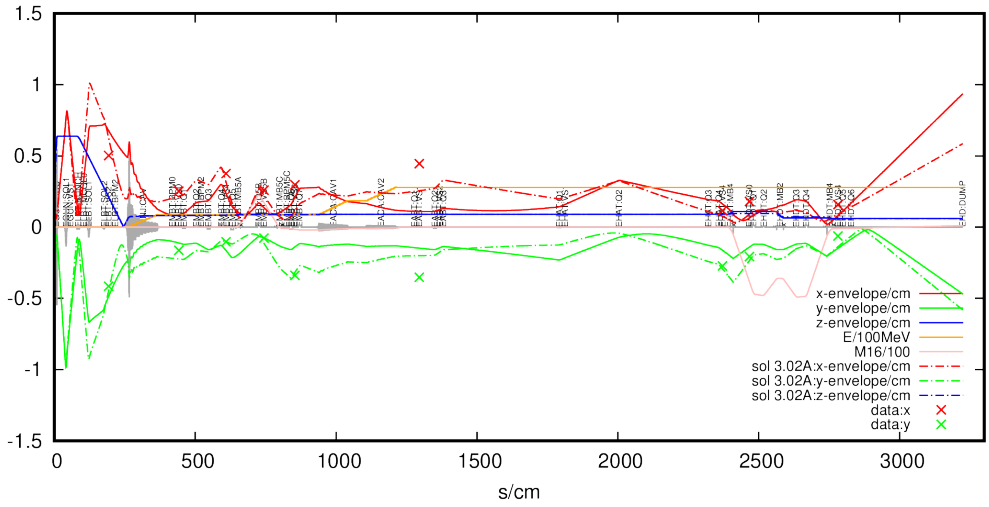

Figure 5: Dashed lines show the beam envelope when EGUN:SOL1 is set to 3.02 A, while the solid line is the envelope using actual solenoid current set to 2.91 A. Crosses are data $\sqrt{5}$-rms envelope taken using real beam.

4 High order aberration from EGUN:SOL1

4.1 Results from GPT

Assuming the normalized beam emittance at the cathode to be about 14 μm (close to the usual value we determined from solenoid scan), the effect of solenoid aberration is further investigated in a multi-particle tracking code: GPT. Tracking was done up to EINJ entrance. The simulation result is compared with TRANSOPTR, where the initial beam conditions

are set to be the same as the beam at the cathode grid in GPT:

$$\begin{aligned}
\sigma_{11} = \sigma_{33} &= \sqrt{5}\sigma_x = 0.417\,\text{cm} \\
\sigma_{22} = \sigma_{44} &= 0.665 \\
\sigma_{55} &= \sqrt{5}\sigma_z = 0.0139\,\text{cm} \\
\sigma_{66} &= \sqrt{5}\sigma_{p_z} = 0.585 \\
\text{r12=}\ \text{r34} &= 0.0 \\
\text{r56} &= 0.51 \\
\text{Average E} &\approx 6\,\text{eV}
\end{aligned}$$

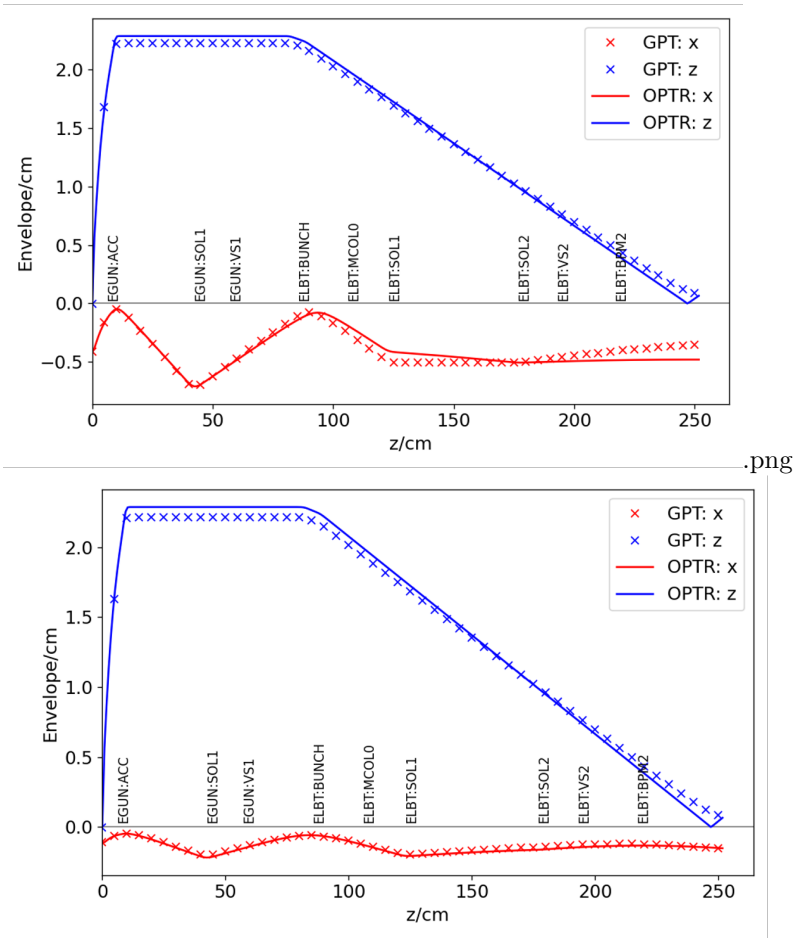

.png

Figure 6: Comparison of the beam envelope for an initial normalized emittance of about 14 μm (top) and 3.5 μm (bottom) respectively.

4.2 Possible Mitigation

Solenoids' axial field can be expanded as follows:

$$B_s = B_s(0,s) - \frac{r^2}{4}\frac{\mathrm{d}^2 B_s(0,s)}{\mathrm{d}s^2} + ... \tag{1}$$

Its aberrations depends on the mean-squared value of $B' = \frac{\mathrm{d}B_s(0,s)}{\mathrm{d}s}$ [2],

$$\Delta r' = -\frac{K}{2} r^3 \int B'^2 \mathrm{d}s \tag{2}$$

It is apparent that solenoids' spherical aberrations diverge in the hard edge limit. The new clamp on this solenoid has a sharper field and harder edge as compared to the old clamp, or even no clamp (Fig. 7). This shows that possible mitigation of the significant aberration in the low-energy section of e-Linac by flattening their fields, i.e. removing the clamp.

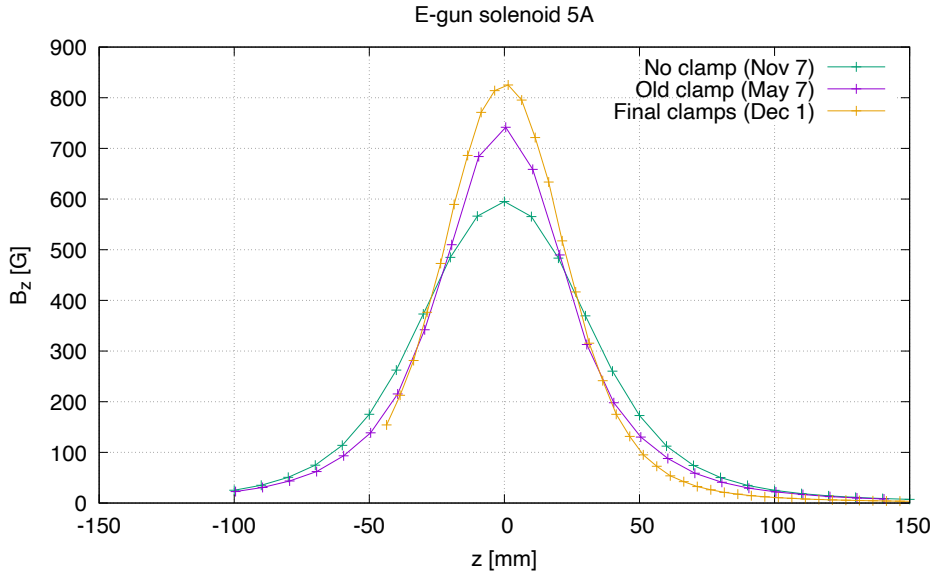

Figure 7: The on-axis magnetic field for EGUN:SOL1 at I=5.0 A for old clamp, new clamp and no clamp respectively.

Fig. 8 shows the result using the no-clamp field (extrapolated to ±250 mm). The coil current of EGUN:SOL1 is increased from 2.91 A to 3.5 A (about 1.2 times) to achieve similarly small beam size at the buncher entrance. Although the effect of aberration is still there, but emittance growth is reduced. For instance, at ELBT:VS2, the ratio of $\frac{\epsilon_{nx}}{\epsilon_{nx0}}$ is reduced from 1.131 to 1.067.

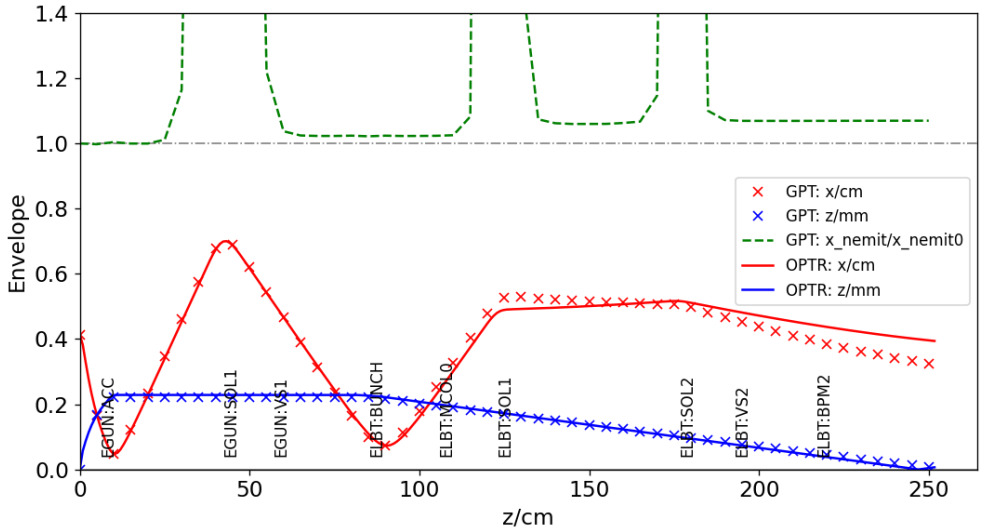

(a) No clamp

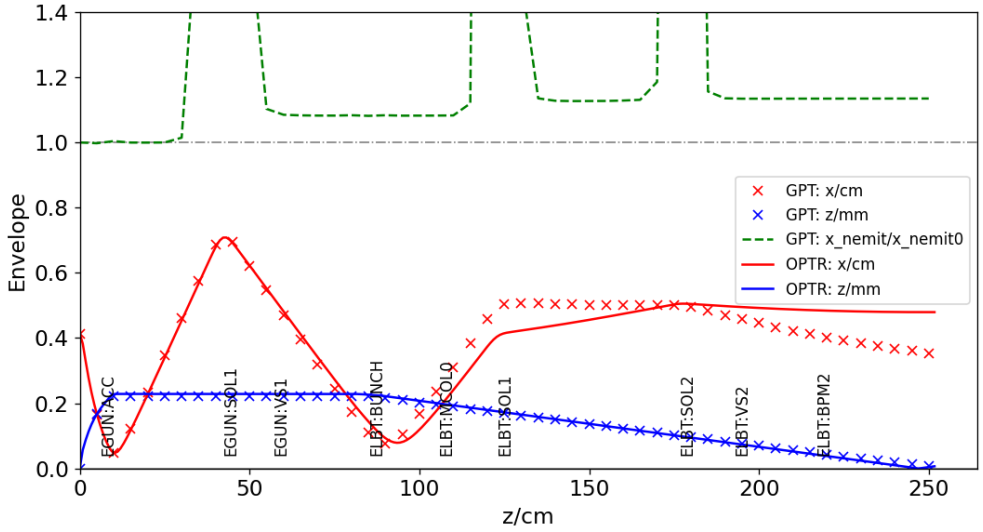

(b) With clamp

Figure 8: The envelope calculated using GPT comparing the effect of the solenoid clamp on the aberration. The green line shows the ratio of the normalized x emittance with respect to its initial value 13.4 μm. The result without clamp shows a smaller effect from the aberration, although its presence remains significant.

References

[1] Kevin Multani. ELBT SN0002 Solenoid, 2014.

[2] Rick Baartman. Envelope codes why. Technical Report TRI-BN-23-14, TRIUMF, 2023. http://lin12.triumf.ca/text/2023Envelope/2023Envelope.pdf.